Supporting Information

Biomineralized Bimetallic Oxide Nanotheranostics for Multimodal Imaging-Guided Combination Therapy

Jianrong Wu[1], Gareth R. Williams[2], Shiwei Niu[1], Yanbo Yang[1], Yu Li[1], Xuejing Zhang[1], Li-Min Zhu[1]✉

[1]College of Chemistry, Chemical Engineering and Biotechnology, Donghua University, Shanghai 201620, P.R. China

[2]UCL School of Pharmacy, University College London, 29-39 Brunswick Square, London WC1N 1AX, UK

✉ Corresponding author: Email addresses: lzhu@dhu.edu.cn (L.-M. Zhu).

Supplementary Figures

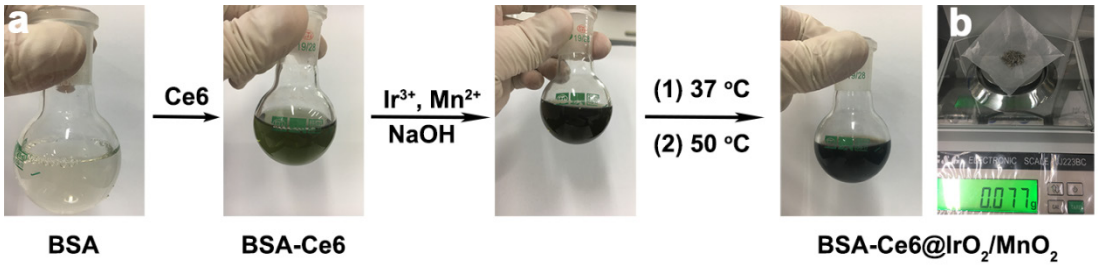

Figure S1. (a) The synthetic process for BSA-Ce6@IrO_2/MnO_2 nanoparticles. (b) A digital photo of the lyophilized BSA-Ce6@IrO_2/MnO_2 nanoparticles.

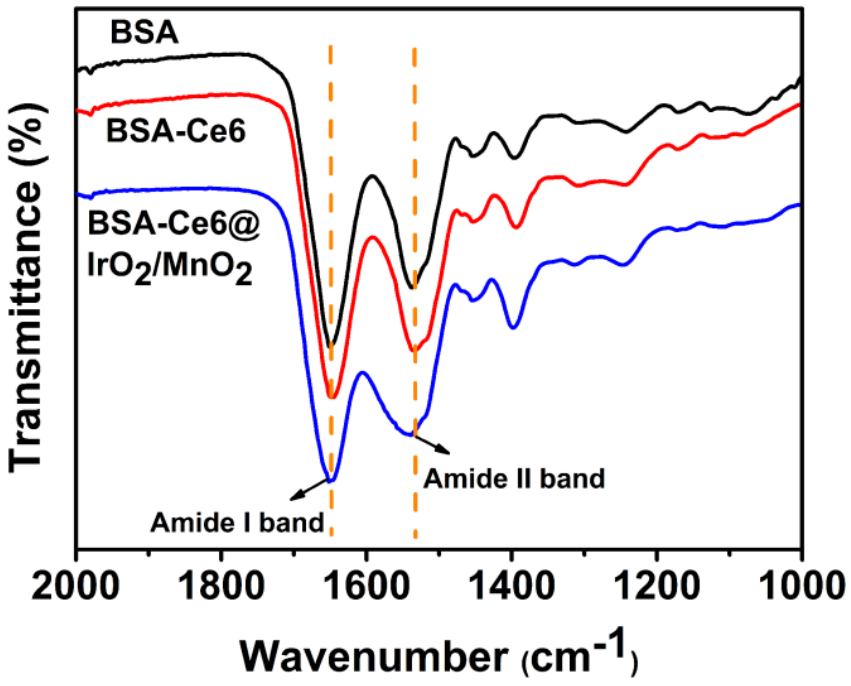

Figure S2. FT-IR spectra of BSA, BSA-Ce6, and BSA-Ce6@IrO_2/MnO_2.

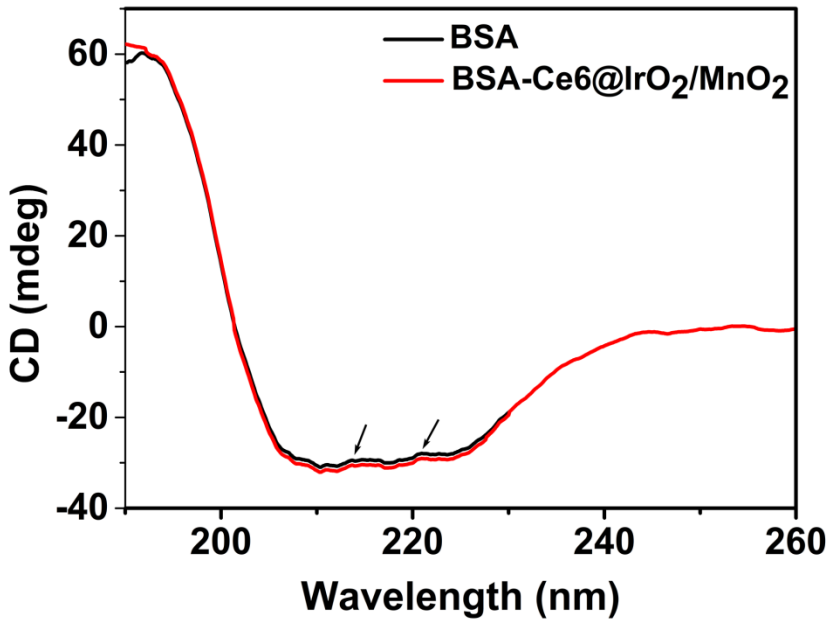

Figure S3. Circular dichroism spectra of BSA and BSA-Ce6@IrO_2/MnO_2.

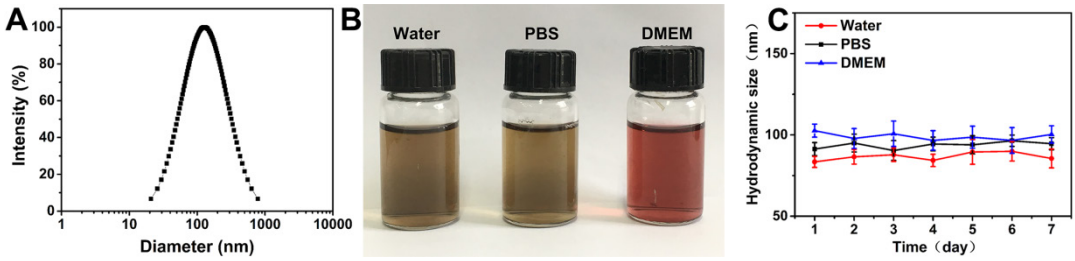

Figure S4. Data on BSA-Ce6@IrO_2/MnO_2 dispersions. (A) The hydrodynamic diameter in PBS. (B) Photographs of the dispersions in water, PBS, and DMEM. (C) The hydrodynamic sizes of the NPs in different media over 7 days.

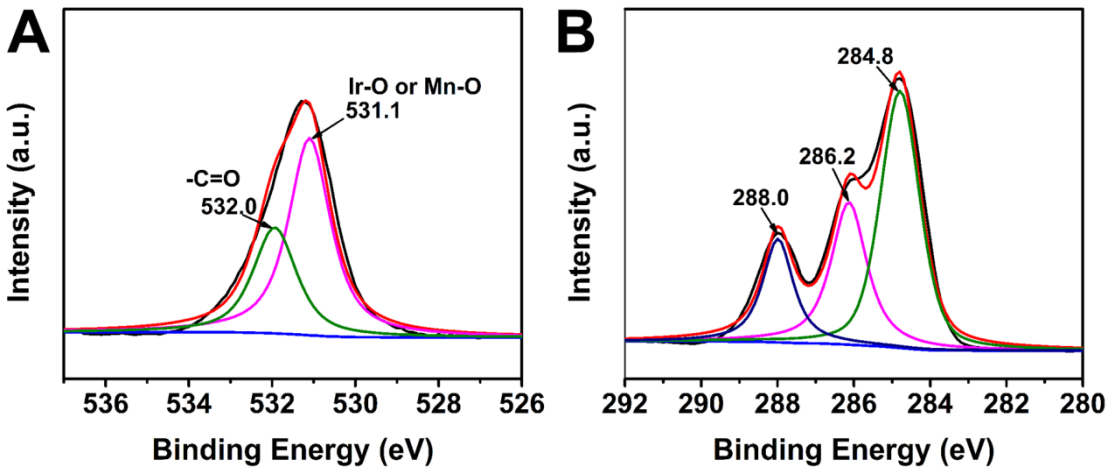

Figure S5. (A) O 1s and (B) C 1s XPS spectra of the BSA-Ce6@IrO_2/MnO_2 nanoparticles.

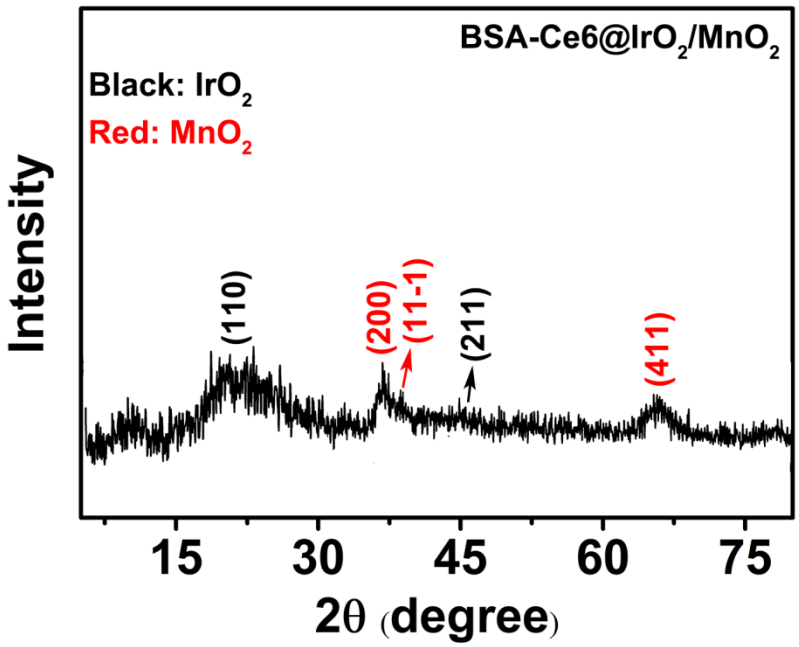

Figure S6. The X-ray diffraction pattern of BSA-Ce6@IrO_2/MnO_2 NPs.

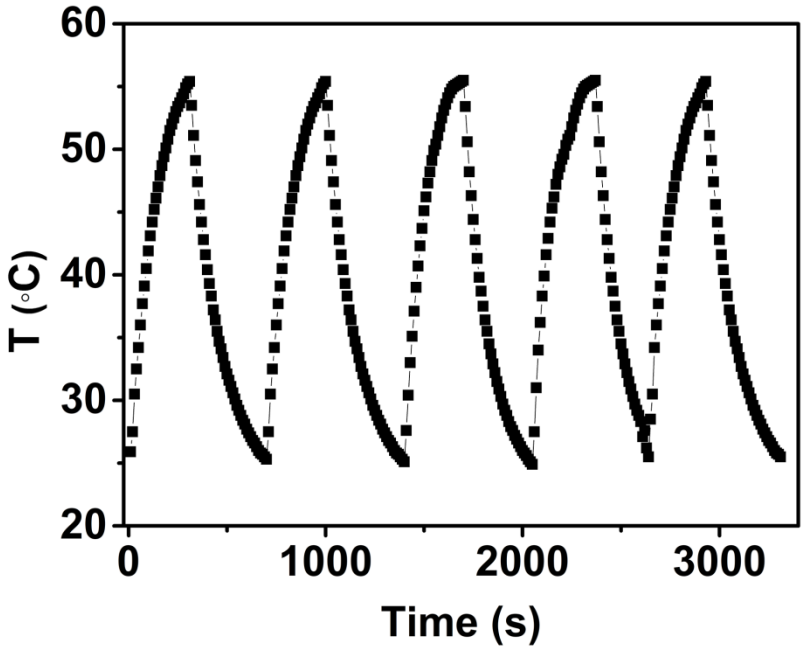

Figure S7. The temperature-time curve for a BSA-Ce6@IrO_2/MnO_2 dispersion (5 mM with respect to Ir) during five laser on/off cycles.

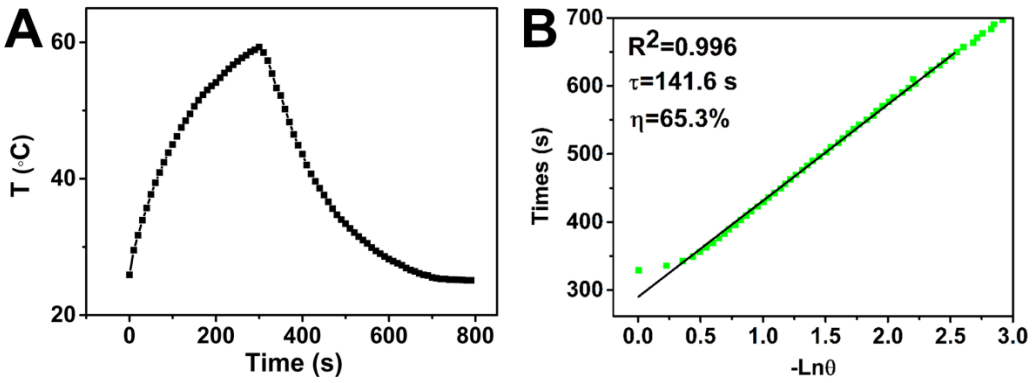

Figure S8. (A) Temperature change of a BSA-Ce6@IrO_2/MnO_2 dispersion (6.0 mM with respect to Ir) irradiated with an 808 nm laser. The laser was turned off after irradiation for 600 s. (B) The time constant for heat transfer of the BSA-Ce6@IrO_2/MnO_2 dispersion, calculated by plotting time data versus ln θ (defined as the ratio of ΔT to ΔT_{max}) during the cooling process.

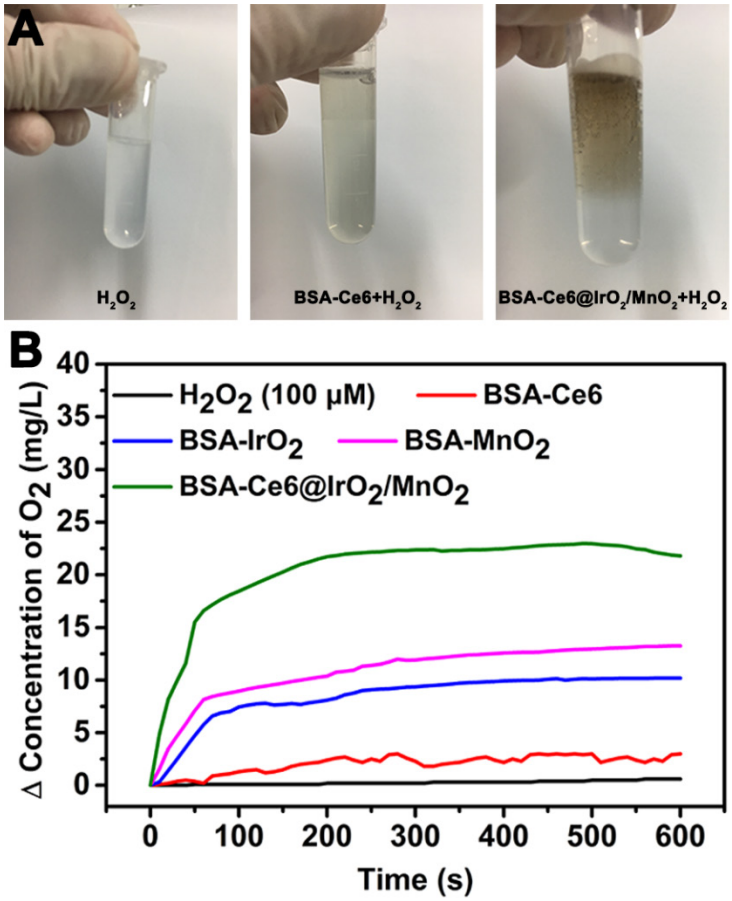

Figure S9. (A) Photographs of H_2O_2 solutions after incubation with BSA-Ce6 or BSA-Ce6@IrO_2/MnO_2 nanoparticles (Ir: 3 mM, Mn: 2 mM). (B) Oxygen generation in H_2O_2 solutions after incubation with BSA-Ce6, BSA-IrO_2 (Ir: 3 mM), BSA-MnO_2 (Mn: 2 mM) or BSA-Ce6@IrO_2/MnO_2 nanoparticles (Ir: 3 mM, Mn: 2 mM).

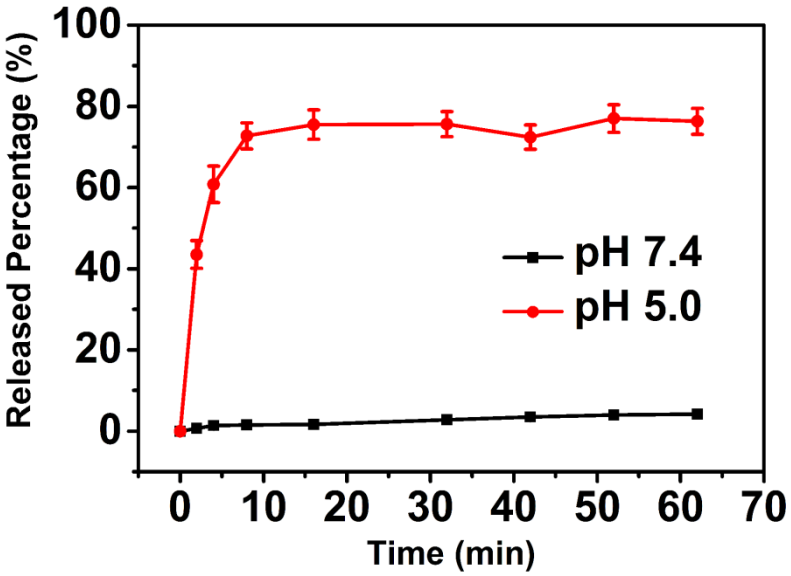

Figure S10. The percentage of Mn^{2+} released from BSA-Ce6@IrO_2/MnO_2 NPs over time in PBS at different pH values (7.4, and 5.0). Results are shown as mean ± S.D. from 6 independent experiments.

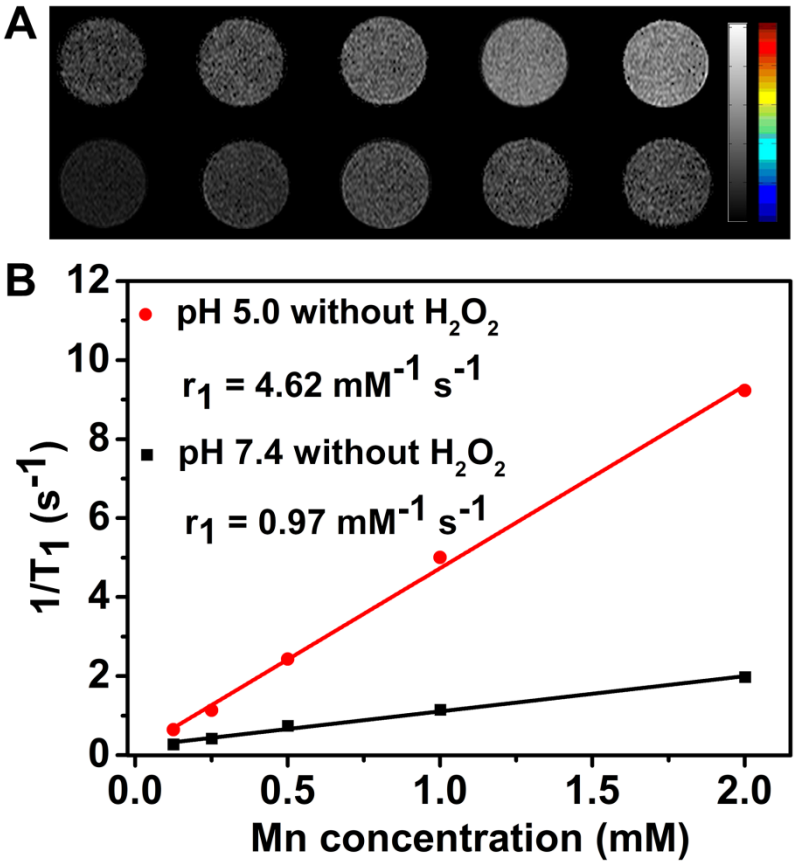

Figure S11. T_1-weighted MR images and relaxivity fits of BSA-Ce6@IrO_2/MnO_2 dispersions at pH 5.0 and 7.4 without H_2O_2.

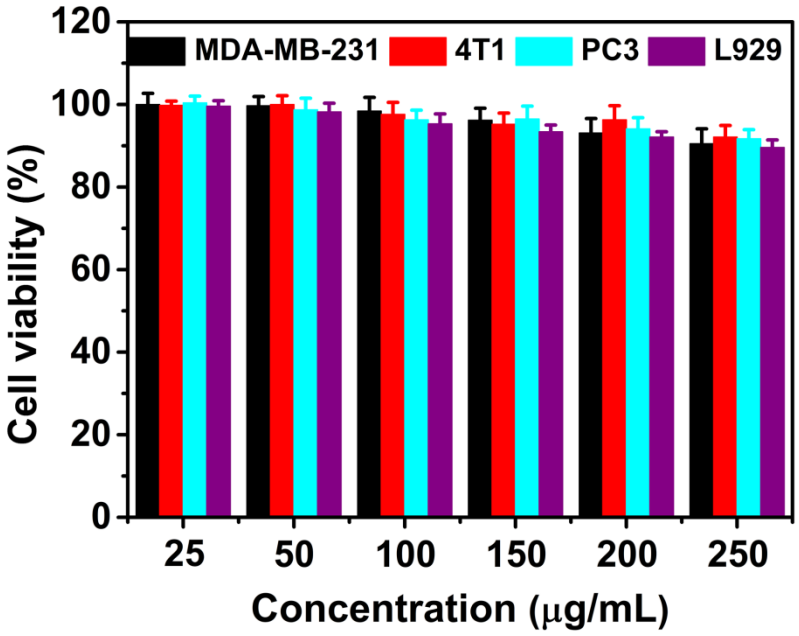

Figure S12. Relative cell viability of MDA-MB-231, 4T1, PC3, and L929 cells after incubation with different concentrations of BSA-Ce6@IrO_2/MnO_2 for 24 h. Values are given as a percentage relative to an untreated cells control (n = 5).

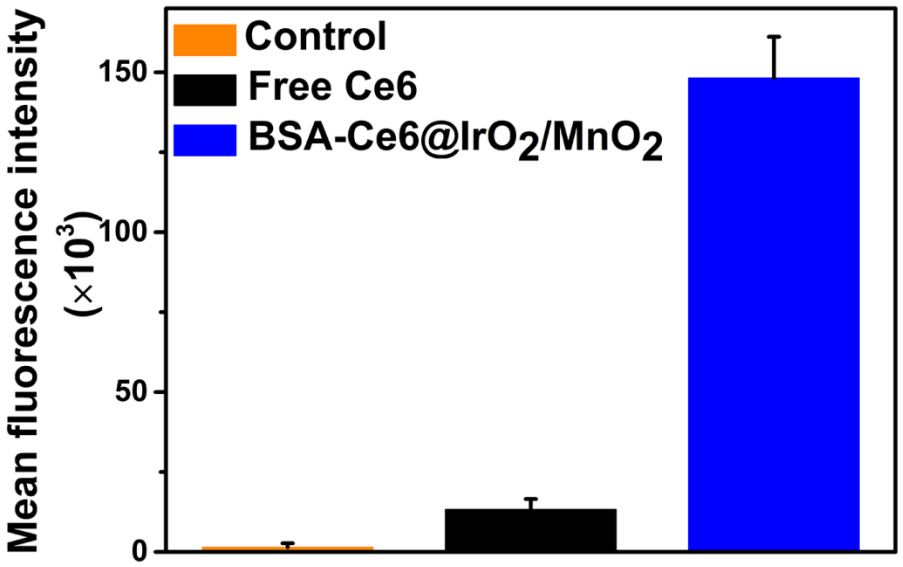

Figure S13. Quantitative mean fluorescence intensities derived from the flow cytometric analysis in Figure 4D (n = 5).

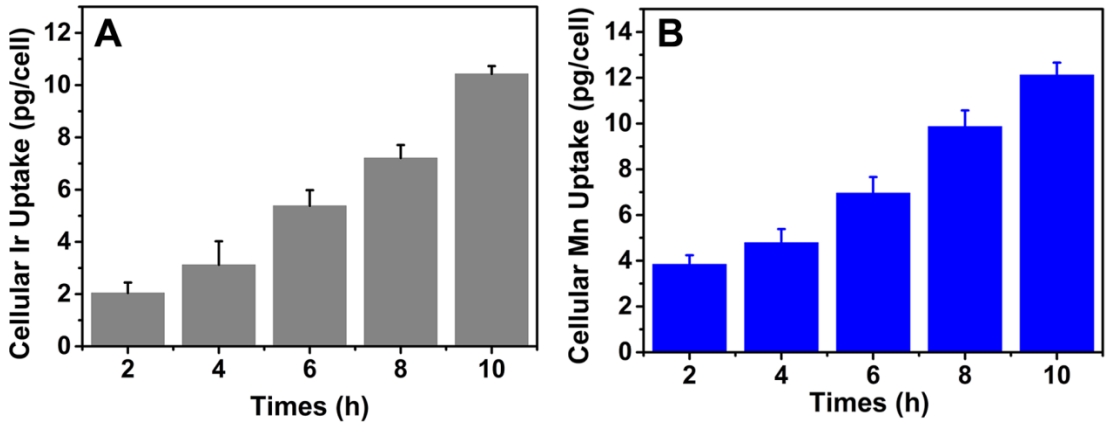

Figure S14. The uptake of (A) Ir and (B) Mn by MDA-MB-231 cells at different times after treatment with the BSA-Ce6@IrO_2/MnO_2 nanoparticles (n = 5).

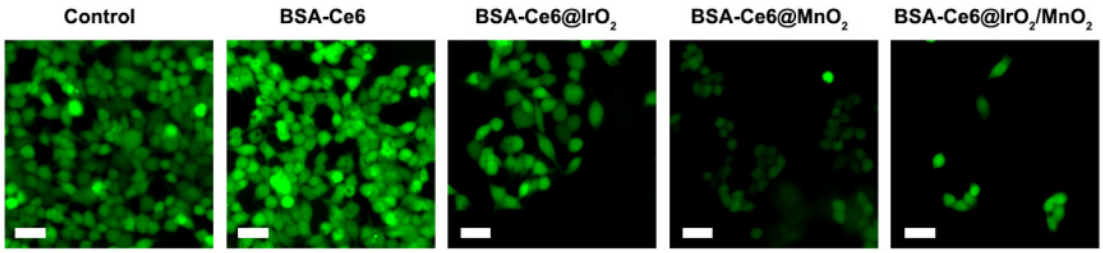

Figure S15. Intracellular O_2 production (as quantified using the RDPP O_2 probe) after MDA-MB-231 cells were incubated with different formulations (Ir: 3 mM, Mn: 2 mM). Scale bars: 50 μm.

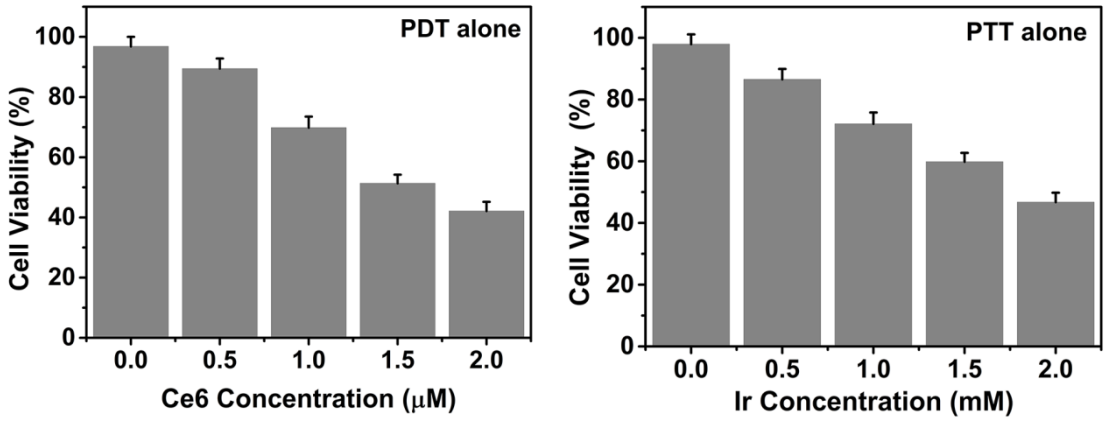

Figure S16. Concentration-dependent cell viability of MDA-MB-231 cells treated with BSA-Ce6@IrO_2/MnO_2. (A) PDT: 660 nm light irradiation (5 mW cm^{-2}, 30 min); (B) PTT: 808 nm (1.0 W cm^{-2}, 10 min).

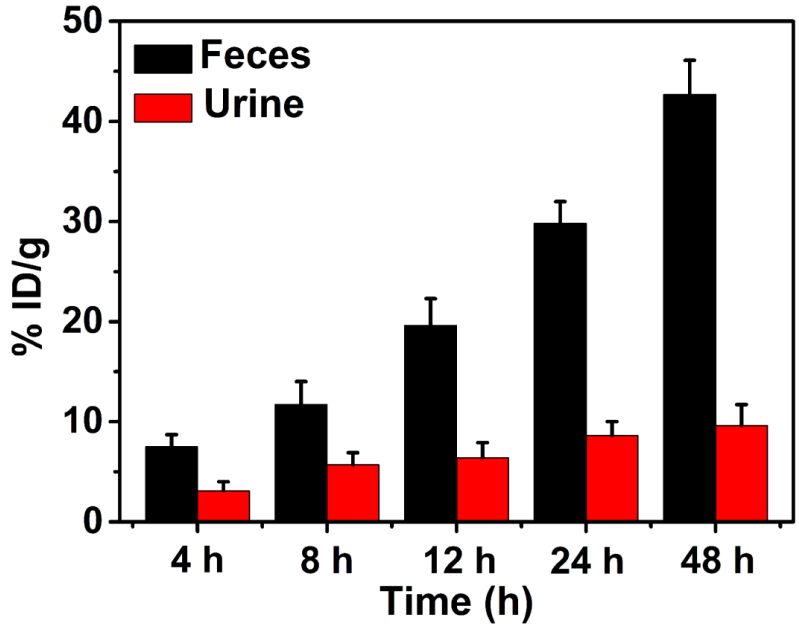

Figure S17. Quantification of BSA-Ce6@IrO_2/MnO_2 nanoparticles in urine and feces of MDA-MB-231 tumor-bearing mice at various time points after injection (n = 4).

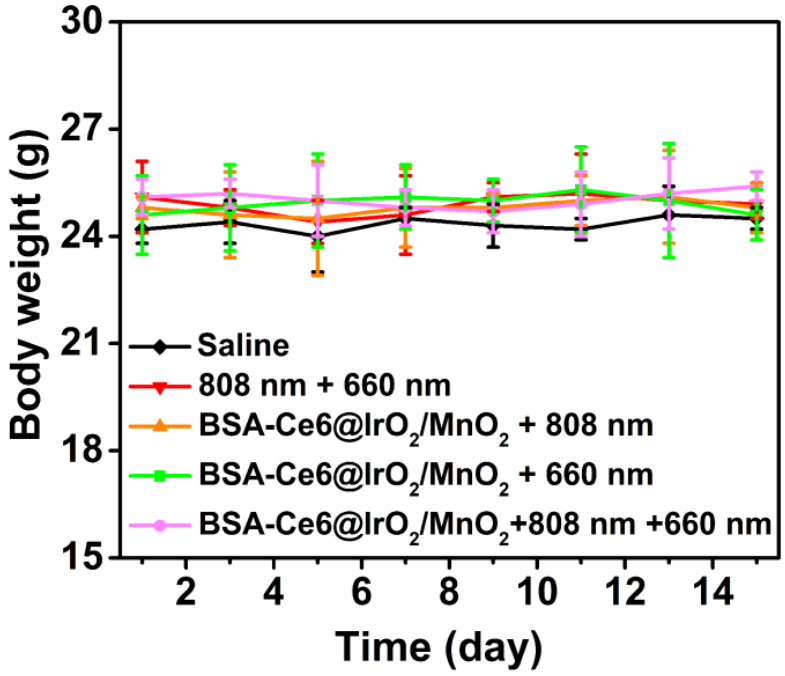

Figure S18. Body weight of MDA-MB-231 tumor-bearing mice during different treatments (n = 4).

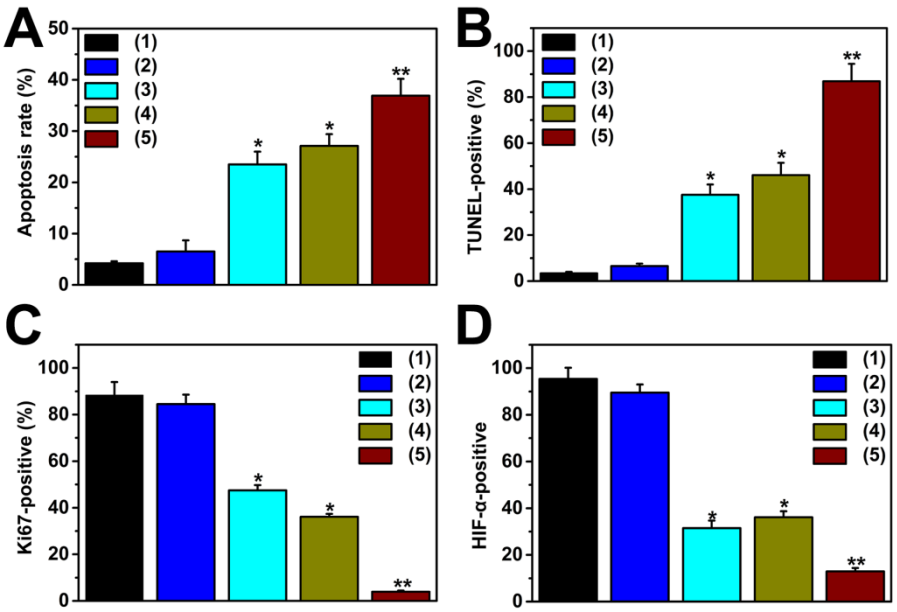

Figure S19. Quantitative analysis of (a) cell apoptosis, (b) TUNEL, (c) Ki67 and (d) HIF-α positive rates after the different *in vivo* treatments. **P < 0.01 and *P < 0.05 by Student's two-tailed t test. Groups are (1) saline, (2) 808 nm + 660 nm laser irradiation, (3) BSA-Ce6@IrO_2/MnO_2 + 808 nm laser, (4) BSA-Ce6@IrO_2/MnO_2 + 660 nm laser, and (5) BSA-Ce6@IrO_2/MnO_2 + 808 nm + 660 nm lasers, respectively.

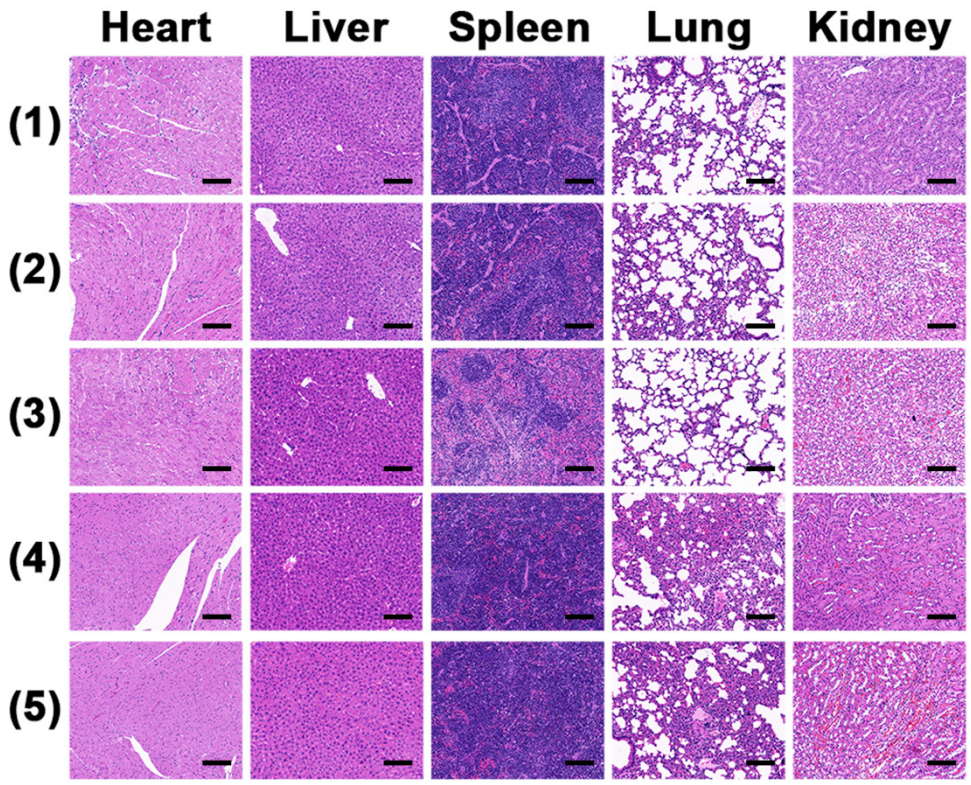

Figure S20. H&E-stained tissue sections of the major organs (heart, liver, spleen, lung, and kidney). Data were collected on day 15 from mice treated with (1) saline, (2) 808 nm + 660 nm laser irradiation, (3) BSA-Ce6@IrO_2/MnO_2 + 808 nm laser, (4) BSA-Ce6@IrO_2/MnO_2 + 660 nm laser, and (5) BSA-Ce6@IrO_2/MnO_2 + 808 nm + 660 nm lasers, respectively. Scale bars: 50 μm.

.

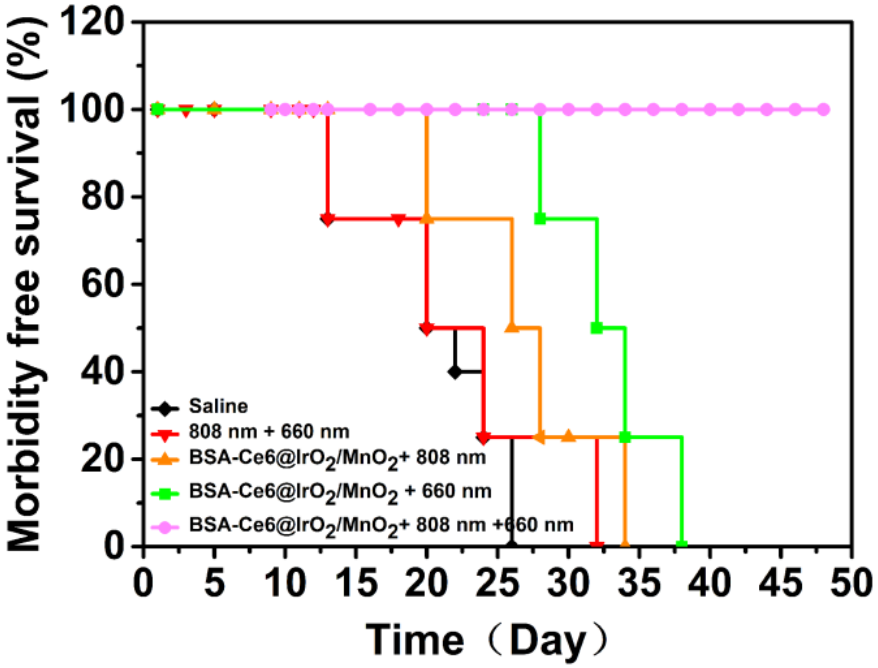

Figure S21. Survival rates of MDA-MB-231 tumor–bearing mice as a function of time post treatment.

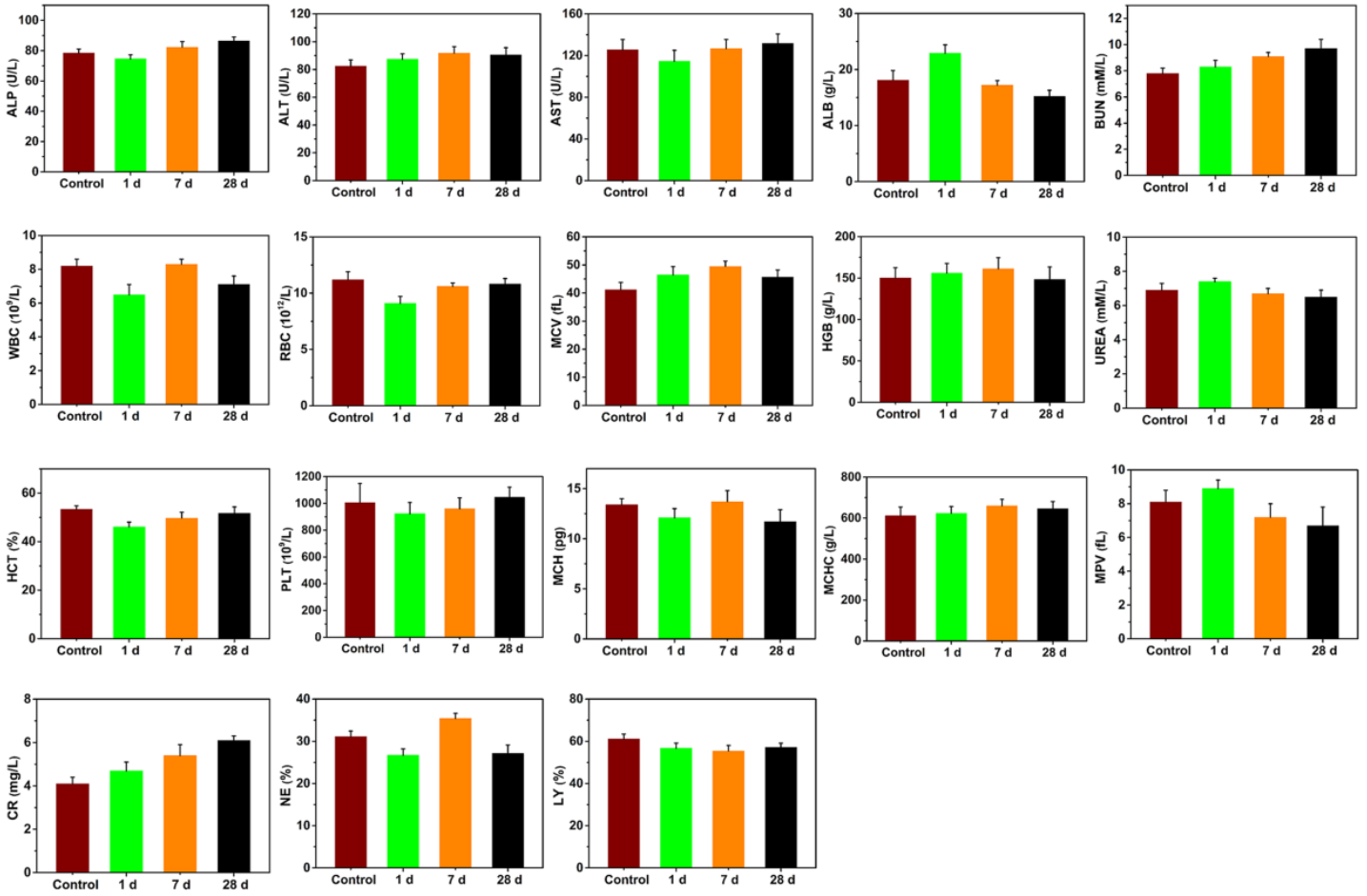

Figure S22. Blood biochemistry and hematology data of Balb/c mice treated with BSA-Ce6@IrO_2/MnO_2 nanoparticles at day 1, 7, and 28 after initial injection (n =4). The control samples are those taken at day 0 before treatment began.

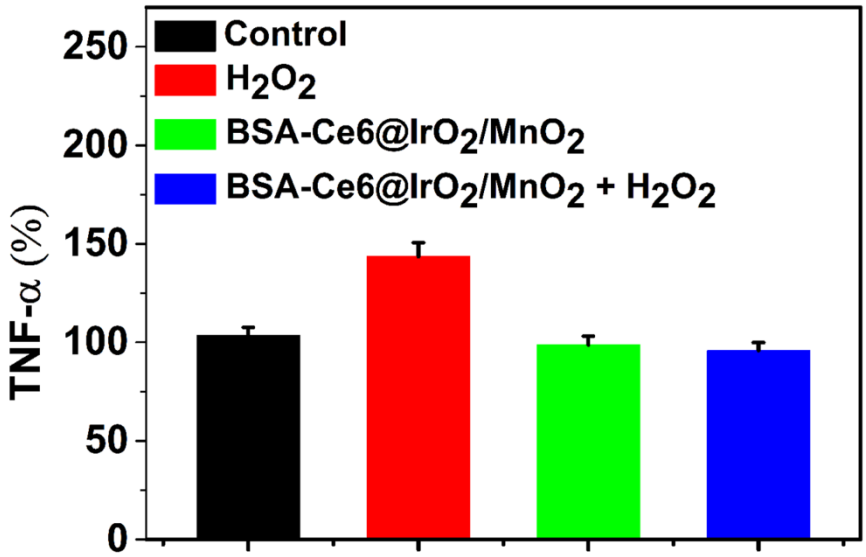

Figure S23. The TNF-α level in the sera of MDA-MB-231tumor-bearing mice after different treatments (n = 5).